HHS Public Access

Author manuscript

Mol Cell. Author manuscript; available in PMC 2017 March 03.

Published in final edited form as:

Mol Cell. 2016 March 3; 61(5): 747–759. doi:10.1016/j.molcel.2016.01.029.

Enhancer of rudimentary cooperates with conserved RNA processing factors to promote meiotic mRNA decay and facultative heterochromatin assembly

Tomoyasu Sugiyama[1], **Gobi Thillainadesan**[1], **Venkata R. Chalamcharla**[1], **Zhaojing Meng**[2], **Vanivilasini Balachandran**[1], **Jothy Dhakshnamoorthy**[1], **Ming Zhou**[2], and **Shiv I.S. Grewal**[1,*]

[1]Laboratory of Biochemistry and Molecular Biology, National Cancer Institute, Bethesda, MD 20892, USA

[2]Laboratory of Proteomics and Analytical Technologies, Frederick National Laboratory for Cancer Research, Frederick, MD 21702, USA

SUMMARY

Erh1, the fission yeast homolog of *Enhancer of rudimentary*, is implicated in meiotic mRNA elimination during vegetative growth, but its function is poorly understood. We show that Erh1 and the RNA-binding protein Mmi1 form a stoichiometric complex called EMC (Erh1-Mmi1 complex), to promote meiotic mRNA decay and facultative heterochromatin assembly. To perform these functions, EMC associates with two distinct complexes, MTREC (Mtl1-Red1 core) and CCR4-NOT. Whereas MTREC facilitates assembly of heterochromatin islands coating meiotic genes silenced by the nuclear exosome, CCR4-NOT promotes RNAi-dependent heterochromatin domain (HOOD) formation at EMC-target loci. CCR4-NOT also assembles HOODs at retrotransposons and regulated genes containing cryptic introns. We find that CCR4-NOT facilitates HOOD assembly through its association with the conserved Pir2/ARS2 protein, and also maintains *rDNA* integrity and silencing by promoting heterochromatin formation. Our results reveal connections among Erh1, CCR4-NOT, Pir2/ARS2 and RNAi, which target heterochromatin to regulate gene expression and to protect genome integrity.

Graphical Abstract

*To whom correspondence should be addressed: grewals@mail.nih.gov.

AUTHOR CONTRIBUTIONS

T.S. and S.I.S.G. designed the experiments; T.S., G.T., V.R.C., Z.M., V.B., J.D. and M.Z. performed the experiments; T.S., G.T., Z.M., M.Z. and S.I.S.G. analyzed the data; T.S. and S.I.S.G wrote the manuscript.

ACCESSION NUMBER

All ChIP-chip and RNA-sequencing datasets can be accessed at the NCBI GEO under the accession code GSE76114.

SUPPLEMENTAL INFORMATION

Supplemental information includes Supplemental Experimental Procedures, 7 Figures and 7 Tables and can be found with this article online.

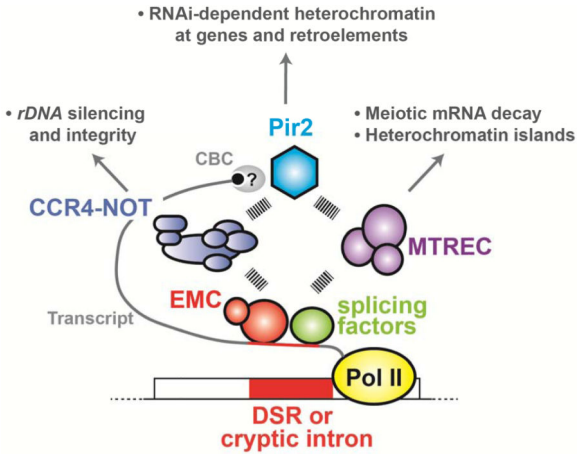

INTRODUCTION

Gametes are produced from germ cells when they undergo meiosis, a complex differentiation process that relies on developmental signaling pathways to direct cell division and reductional chromosome segregation. The fission yeast *Schizosaccharomyces pombe* is an excellent system for studying meiosis (Yamamoto, 1996a). In fission yeast, cells respond to nitrogen starvation by switching from the mitotic cell cycle to meiotic sexual differentiation, which in turn triggers pheromone production and response, cell conjugation and meiosis to occur in sequential order. Completion of meiosis in diploid cells requires Mei2, a master regulator of meiosis. Mei2 is normally targeted for degradation in vegetative cells through phosphorylation by the Pat1 kinase. However, the expression of Mei3, which is a pseudo-substrate for the Pat1 kinase, inhibits Pat1 activity in conjugated cells, resulting in Mei2 stabilization. Mei2 then binds to meiRNA, a meiosis-specific non-coding RNA encoded by the *sme2*$^{+}$ gene, to form a nuclear dot. This Mei2-meiRNA ribonucleoprotein complex is believed to facilitate the transcription of various meiosis-specific genes that are essential to complete meiosis in diploid cells (Yamamoto, 1996b).

Recent advances have now dispelled the long held belief that meiotic gene transcription is active only in meiotic *S. pombe* cells. Meiotic gene transcription does occur in vegetative cells, but meiotic mRNAs are selectively eliminated from mitotically dividing cells to prevent their inappropriate expression (Harigaya et al., 2007; Yamamoto, 1996a). This mRNA elimination system specifically degrades transcripts that contain a DSR (determinant of selective removal) element and a polyadenylated tail (Harigaya et al., 2006; Yamanaka et al., 2010). The DSR core sequence (UCAAAC or UUAAAC) in meiotic mRNAs is recognized by the YTH domain-containing protein Mmi1, which in turn engages various proteins such as MTREC, composed of the Zn-finger protein Red1 and the Mtr4-like RNA helicase Mtl1, as well as MTREC-associated factors including the serine and proline-rich protein Pir1/Iss10, the Zn-finger protein Red5, the nuclear poly(A)-binding protein Pab2, the canonical poly(A) polymerase Pla1 and the nuclear exosome, to degrade target mRNAs (Chen et al., 2011; Egan et al., 2014; Lee et al., 2013; St-Andre et al., 2010; Sugiyama and Sugioka-Sugiyama, 2011; Sugiyama et al., 2013; Yamanaka et al., 2010; Yamashita et al., 2012; Yamashita et al., 2013; Zhou et al., 2015).

In addition to elimination of meiotic mRNAs during vegetative growth, DSR-dependent mRNA degradation machinery also promotes the assembly of facultative heterochromatin at discrete regions in the *S. pombe* genome (Hiriart et al., 2012; Tashiro et al., 2013; Yamanaka et al., 2013; Zofall et al., 2012). These regions include RNAi-independent heterochromatin islands formed at meiotic genes (e.g., *mei4*$^+$ and *ssm4*$^+$), and RNAi-dependent HOODs, which are heterochromatin domains formed at meiotic genes (e.g., *mug5*$^+$ and *mcp3*$^+$), genes regulated by environmental cues (e.g., *pho1*$^+$), and retrotransposons (Cam et al., 2005; Shah et al., 2014; Yamanaka et al., 2013; Zofall et al., 2012). HOODs are particularly evident under specific growth conditions or when the nuclear exosome subunit Rrp6 is deleted (Yamanaka et al., 2013). The assembly of heterochromatin islands and HOODs is coordinated by distinct MTREC-associated factors. For example, Pir1 assembles heterochromatin islands, whereas Pla1 and Pab2 direct the formation of HOODs (Lee et al., 2013; Yamanaka et al., 2013). However, the detailed mechanism by which the RNA elimination system directs heterochromatin assembly at different sites in the genome is not yet fully established.

The *S. pombe* protein Erh1 (*Enhancer of rudimentary* homolog 1) is essential for the suppression of meiotic mRNAs during vegetative growth and for normal cell growth (Krzyzanowski et al., 2012; Yamashita et al., 2013). The gene was first identified in *Drosophila* as a mutation that enhances the wing phenotype of hypomorphic *rudimentary* mutations, and was named *enhancer of rudimentary* (Wojcik et al., 1994). The encoded product ERH is a small protein, and highly conserved orthologs are found in most eukaryotes (Weng and Luo, 2013). ERH has been shown to be critical for cell growth and is implicated in multiple processes such as CENP-E splicing in humans (Weng and Luo, 2013).

Here we investigate the role of Erh1 in meiotic mRNA degradation and heterochromatin assembly. Interestingly, we find Erh1 and Mmi1 form a tight complex, which we term EMC (Erh1-Mmi1 complex). EMC promotes meiotic mRNA decay and heterochromatin assembly in distinct ways. In addition to directing MTREC-mediated mRNA decay and the formation of heterochromatin islands at meiotic genes silenced by the exosome, EMC engages CCR4-NOT for RNAi-dependent assembly of HOODs. CCR4-NOT also promotes *rDNA* silencing and integrity, and triggers RNAi-mediated heterochromatin assembly at genes and retrotransposons containing cryptic introns. Importantly, our analyses suggest that CCR4-NOT cooperates with Pir2/Ars2, which is known to associate with the nuclear Cap-binding complex, to facilitate small RNA production and heterochromatin formation. These results provide important insights into pathways governing RNA decay and facultative heterochromatin assembly in different parts of the genome.

RESULTS

Erh1 colocalizes with nuclear RNA degradation machinery

Erh1 localizes to the nucleus (Krzyzanowski et al., 2012), but its in-depth characterization has been lacking. In vegetative cells, we found that GFP-tagged Erh1 was evenly distributed in chromatin regions, which were visualized by co-expressing CFP-tagged histone H3 (Hht1); additionally, Erh1 formed nuclear foci that were often located at the edges of

chromatin domains (Figure 1A). Moreover, we found that Erh1 colocalized with foci formed by known nuclear factors involved in meiotic mRNA decay, including Red1, Mtl1 and Rrp6, as well as with Pcf11, a cleavage and polyadenylation specificity factor (Figure 1B). Thus, we find that Erh1 colocalizes with RNA elimination factors to cleavage bodies in vegetative cells.

Loss of Erh1 causes growth defect and mating deficiency

To further understand the functions of Erh1, we generated and characterized an *erh1*Δ strain. The *erh1*Δ strain carrying the *ade6-M210* or *ade6-M216* allele displayed pink and pale pink colony color on adenine-limiting medium, as compared to red and pink colonies formed by WT cells carrying *ade6-M210* or *ade6-M216*, respectively (Figures S1A). In addition, *erh1*Δ cells displayed a growth defect and cold sensitivity (Figures S1B). These phenotypes consistently segregated with *erh1* (Figures S1A and S1B). We next tested if the growth defect may result from the ectopic expression of meiotic mRNAs. Since the lethality of *mmi1*Δ can be rescued by the deletion of the meiotic gene *mei4*$^{+}$ (Harigaya et al., 2006), we asked whether *erh1*Δ growth defects were also suppressed by *mei4*Δ. Interestingly, the growth defects observed in *erh1*Δ at both 30°C and 19°C were suppressed by *mei4*Δ. In contrast, *mei4*Δ failed to rescue the growth defect or the cold sensitivity caused by *red1*Δ (Figure S1C). This result indicates that Mei4 shows a specific genetic interaction with Erh1, but not with Red1, even though both Erh1 and Red1 are required for suppression of *mei4* mRNA (Sugiyama and Sugioka-Sugiyama, 2011; Yamashita et al., 2013).

We also noticed that *erh1*Δ cells displayed a severe mating defect. When meiosis is induced, homothallic (*h*^{90}) wild-type cells sporulate and form asci. These asci can be detected by exposure to iodine vapor, which stains the starch-like compound in the spore wall. However, *erh1*Δ cells showed decreased intensity of iodine staining and a reduced mating efficiency (74.5% for WT and 15.8% for *erh1*Δ) (Figure 1C). Interestingly, we also observed a weak iodine staining in non-switching *erh1*Δ cells (Figure S1D). Since we did not observe haploid meiosis in non-switching *erh1*Δ cells by microscopy (data not shown), the weak iodine staining implies that *erh1*Δ may affect meiotic gene expression and result in ectopic starch accumulation in haploid cells during nitrogen starvation.

Erh1 is required for DSR-mediated mRNA decay

Four meiotic mRNAs containing the DSR sequence (*mei4*, *rec8*, *ssm4* and *spo5*) accumulate in *erh1*Δ cells (Yamashita et al., 2013), suggesting that DSR-dependent mRNA decay requires Erh1. To confirm that Erh1 is indeed required for DSR-dependent mRNA decay, we combined *erh1*Δ with the *ura4*$^{+}$-DSR construct (Harigaya et al., 2006), which comprises the *ura4*$^{+}$ gene fused to the *mei4*$^{+}$ DSR region (Figure 1D, top). We found that *erh1*Δ as well as *red1*Δ carrying *ura4*$^{+}$-DSR grew on medium lacking uracil (Figure 1D, bottom), indicating that Erh1 is essential for DSR-directed mRNA degradation in vegetative cells.

Erh1 suppresses meiotic genes in vegetative cells

To gain insight into the target transcripts of Erh1, we analyzed the expression profile of vegetative WT and *erh1*Δ strains using RNA-Seq. We identified 602 transcripts that were upregulated >2-fold in vegetative *erh1*Δ relative to WT cells (Table S1). Of the 602

transcripts, 223 transcripts were previously shown to increase during nitrogen starvation or meiosis (Wilhelm et al., 2008). For example, DSR-containing mRNAs such as *mei4* and *ssm4* were increased in *erh1*Δ (Figure 2A), which is consistent with a previous report (Yamashita et al., 2013). We classified the 223 transcripts into 6 categories based on their expression profiles (Mata et al., 2002), and found that many of the upregulated genes are "early" or "middle" meiotic genes (Figure S2A and Table S1). Consistent with this meiotic gene classification, GO (gene ontology) analysis indicated that genes involved in meiotic nuclear division or meiotic cell cycle progression were upregulated in *erh1*Δ (Figure S2B and Table S1). In addition to meiosis-related genes, various types of non-coding RNAs (ncRNAs) also accumulated in *erh1*Δ (Figure S2C and Table S1). These included ncRNAs whose expression is regulated by the environmental growth conditions or developmental signals. For example, the loss of Erh1 caused upregulation of long ncRNA upstream of the phosphate-responsive *pho1*$^+$ and *tgp1*$^+$ genes (Figure 2B), which are regulated by RNA processing factors including Mmi1 and MTREC-associated factors (Ard et al., 2014; Chen et al., 2011; Lee et al., 2013; Shah et al., 2014). These results demonstrate that Erh1 is required for the suppression of meiotic genes and many ncRNAs.

We also identified 356 transcripts with lower steady-state levels (<0.5-fold reduction) in *erh1*Δ than in WT (Table S2). Only 13 were meiotic genes (Figure S2D), in contrast to the large fraction of meiotic genes found among upregulated transcripts. Only a few meiosis-related genes were decreased in *erh1*Δ (Figure S2E). Instead, most of the decreased transcripts, 290 of 356 (81%), represented various ncRNAs, including antisense RNAs, intergenic RNAs, tRNAs, and 5S rRNA (Figure S2F).

Erh1 shares target transcripts with Mmi1 and Red1

We addressed whether Erh1, Red1 and Mmi1 target a common set of transcripts by looking for any overlap among the Red1, Mmi1 and Erh1 regulons. We determined gene expression levels in *erh1*Δ relative to WT, and compared the results with similar analyses of the *red1*Δ and *mmi1*Δ transcriptome profiles. We found significant overlap between Erh1-regulated genes and Red1-regulated genes. Specifically, 246 of 602 transcripts (41%) that were upregulated in *erh1*Δ were also upregulated in *red1*Δ ($p< 4.14\times10^{-67}$) (Figure 2C, right), whereas 43 of 356 transcripts (12%) that were downregulated in *erh1*Δ were also downregulated in *red1*Δ ($p< 5.54\times10^{-29}$) (Figure 2D, right). Interestingly, the overlap between the set of Erh1-regulated genes and Mmi1-regulated genes was even more pronounced: 370 of 602 transcripts (62%) that were upregulated in *erh1*Δ were also upregulated in *mmi1*Δ ($p< 1.86\times10^{-200}$) (Figure 2C, left), whereas 116 of 356 transcripts (33%) that were downregulated in *erh1*Δ were also downregulated in *mmi1*Δ ($p< 4.89\times10^{-100}$) (Figure 2D, left). These results indicate that in vegetative cells, Erh1 regulates the expression of target transcripts that are shared with Red1 and Mmi1, but also that Erh1 function is more closely related to Mmi1 than to Red1.

Erh1 colocalizes with the Mei2-meiRNA dot and Is required for Its formation

We next determined the localization of Erh1 during meiosis. In vegetative cells, Erh1 was evenly distributed in the nucleoplasm and formed nuclear foci (Figures 1A and 3A). Upon meiotic induction, Erh1 converged into a single distinct dot (Figure 3A). In asci, the Erh1

signal coincided with histone H3, but Erh1 foci in spores were not as obvious as in mitotically growing cells (Figure 3A).

The localization patterns we observed for Erh1 were reminiscent of Mmi1, which colocalizes with Mei2-meiRNA, a ribonucleoprotein essential for meiosis (Yamamoto, 1996b), during early meiosis (Ding et al., 2012; Harigaya et al., 2006). As shown in Figure 3B, mCherry-tagged Erh1 (Erh1-mCherry) also colocalized with GFP-tagged Mei2 (Mei2-GFP) and with meiRNA, which was visualized using the MS2-GFP system (Shichino et al., 2014), indicating that Erh1 colocalizes with Mmi1 and meiRNA in meiotic cells.

Mmi1 dots converge during early meiosis in *mei4*Δ, but this convergence does not occur in *mei2*Δ or in *sme2*Δ (*sme2*$^{+}$ encodes meiRNA) (Harigaya et al., 2006; Sugiyama and Sugioka-Sugiyama, 2011). Similarly, we observed a single Erh1 focus in *mei4*Δ, and two Erh1 dots in *mei3*Δ and *sme2*Δ (Figure S3A). Since Mei2 cannot be active in *mei3*Δ (Yamamoto, 1996b), these observations suggest that the formation of the Erh1 single dot requires both Mei2 and meiRNA. We next conversely asked whether Mei2 dot formation requires Erh1. The lack of a Mei2 dot in *erh1*Δ (Figure 3C) indicates that Erh1 facilitates proper Mei2 localization. In addition to Mei2, the meiRNA dot was rarely observed in *erh1*Δ: only 1% (1 out of 75 cells examined) of *erh1*Δ cells had a meiRNA dot, in contrast to 93% (71 out of 73 cells examined) of WT cells (Figures 3D and 3E). In contrast, we found an increased number of *red1*Δ cells either without a meiRNA dot (27.7% vs 2.7%) or with two meiRNA dots (10.6% vs 1.3%), and a large fraction of *red1*Δ cells (61.7%) had a single meiRNA dot (Figures 3D and 3E). Moreover, we noticed that haploid *red1*Δ cells often had a single dot (Figure S3B). These results indicate that unlike Red1, Erh1 and Mmi1 are essential for meiRNA dot formation.

Erh1 and Mmi1 form a complex called EMC

Our findings together with previous studies (Harigaya et al., 2006; Shichino et al., 2014) strongly suggest that the role of Erh1 closely reflects that of Mmi1. To investigate whether Erh1 interacts with Mmi1, we purified Erh1-GFP and found two distinct protein bands of approximately 55 and 39 kDa specifically in the Erh1-GFP purified fraction (Figure 4A). The intensity of the bands indicated that the proteins co-purified in stoichiometric amounts. Mass-spectrometry analyses revealed that the 39 kDa protein was Erh1-GFP, consistent with Western blot results (Figure S4A), and that the 55 kDa protein was Mmi1 (Figure 4A and Table S3). Because Mmi1 associates with both target mRNAs and chromatin (Hiriart et al., 2012; Tashiro et al., 2013), we included a Benzonase treatment step to remove all forms of DNA and RNA during the Erh1-GFP purification. As shown in Figure 4B, Benzonase treatment did not disrupt the interaction between Erh1 and Mmi1, and mass-spectrometry analyses indicated that Erh1 maintained its association with Mmi1 (Table S4). These data indicate that in vegetative cells, Erh1 stoichiometrically and directly associates with Mmi1 to form EMC.

EMC interacts with two distinct protein complexes, MTREC and CCR4-NOT

In addition to Mmi1, other proteins were co-purified with Erh1-GFP including MTREC components Red1 and Mtl1 as well as Pir1/Iss10 (Figure 4A and Table S3). The interaction

between EMC and MTREC is consistent with previous reports of Mmi1 co-purification with Red1 and Mtl1 (Egan et al., 2014; Lee et al., 2013; Zhou et al., 2015). Interestingly, all of the conserved subunits of the CCR4-NOT complex (Miller and Reese, 2012) were also co-purified. Caf4 and Caf16, also annotated as CCR4-NOT subunits, were not found in the Erh1 purified fraction, and are apparently missing from CCR4-NOT in higher eukaryotes. Purification of Ccr4-GFP from *S. pombe* revealed that EMC, MTREC and Pab2 were co-purified with CCR4-NOT (Figure S4B), further confirming the interaction between EMC and CCR4-NOT. Moreover, the association of Erh1 with MTREC and CCR4-NOT was retained after Benzonase treatment, whereas the recovery of RNA-binding proteins such as Vgl1 and Pabp was substantially reduced (Figure 4B and Table S4), indicating that EMC directly engages two distinct protein complexes, MTREC and CCR4-NOT.

We next asked whether the interaction with Mmi1 is required for Erh1 to interact with its partner proteins. To address this, we purified Erh1 from *mmi1*Δ. Although the steady-state level of Erh1-GFP was not affected in *mmi1*Δ (Figure S4C), staining of the fractions revealed that several bands were missing (Figure 4C). Mass-spectrometry analysis revealed that in the absence of Mmi1, MTREC and CCR4-NOT were not recovered with Erh1 (Figure 4C and Table S5), indicating that the integrity of EMC is essential for its interactions with MTREC and CCR4-NOT.

The localization of Erh1 and Mmi1 is mutually dependent

We found Erh1 colocalized with Mmi1 in both vegetative and meiotic cells (Figure 4D), further supporting the notion that Erh1 and Mmi1 form a stable complex. In addition, we observed that Erh1 foci were lost in *mmi1*Δ, and Mmi1 foci were not evident in *erh1*Δ (Figures S4D and S4E). Since the steady-state level of Erh1 or Mmi1 did not change upon deletion of $mmi1^{+}$ or $erh1^{+}$, respectively (Figures S4C and S4F), these results indicate that the assembly of EMC is a prerequisite for its proper localization.

Unlike the loss of Mmi1, the loss of Red1 did not greatly change the level of Erh1-GFP or alter its localization (Figures S4G and S4H). Moreover, *erh1*Δ affected neither the Red1 protein level nor Red1 localization (Figures S4I and S4J). These results indicate that although Erh1 and Red1 colocalize and interact with each other, they are present in distinct functional modules, EMC and MTREC, respectively, which have both separate and overlapping functions. Indeed, MTREC affects several loci that are not regulated by Mmi1 (Lee et al., 2013; Yamanaka et al., 2013)

Erh1 directs the assembly of heterochromatin islands

In addition to constitutive heterochromatin assembled at centromeres, telomeres and the mating-type (*mat*) locus, discrete blocks of heterochromatin islands are found throughout the *S. pombe* genome (Cam et al., 2005; Zofall et al., 2012). Many heterochromatin islands are formed at meiotic genes, and are assembled in a Red1-dependent manner (Egan et al., 2014; Lee et al., 2013; Tashiro et al., 2013; Zofall et al., 2012). Since both Erh1 and Red1 play a role in meiotic mRNA decay, we predicted that Erh1 is also required for the assembly of heterochromatin islands. As expected, we found that dimethylated lysine 9 of histone H3 (H3K9me2), which is a hallmark of heterochromatin, was lost in *erh1*Δ and *mmi1*Δ, and that

both Erh1 and Mmi1 localized to Red1-dependent heterochromatin islands (Figure 5). ChIP followed by quantitative PCR (ChIP-qPCR) analyses confirmed that at two heterochromatin islands, *mei4* and *ssm4*, H3K9me2 levels were greatly reduced in *erh1*Δ and *mmi1*Δ, whereas H3 occupancy levels were not affected (Figure S5A). This result indicates that H3K9me2, but not H3, was reduced at these loci in *erh1*Δ and *mmi1*Δ. In contrast to these heterochromatin islands, constitutive heterochromatin domains were unaffected by the deletion of either $erh1^+$ or $mmi1^+$, and neither Erh1 nor Mmi1 appeared to localize to these regions (Figure S5B). These results demonstrate that EMC is essential for Red1-dependent assembly of heterochromatin islands.

EMC associates with several loci in a heterochromatin-independent manner

In addition to heterochromatin islands, EMC also localized to several loci with no detectable H3K9me2 such as at non-coding RNAs (ncRNAs) located upstream of $byr2^+$ and $tgp1^+$ (Figures S5C and S5D). We found that Erh1 localization to two ncRNA loci, *SPNCRNA.1197* and *SPNCRNA.1459*, was dependent on Mmi1, but not Red1 or Ccr4 (Figure S5E). EMC also associated with $rpl3002^+$ and genes encoding other ncRNAs such as snoRNAs and meiRNA (Figure S5F). Since most of these genes were upregulated in *erh1*Δ, *mmi1*Δ (Table S1), and other RNA elimination factor mutants (Lee et al., 2013), it is likely that EMC and MTREC associate with these genes to target their transcripts for degradation or processing.

Erh1 and CCR4-NOT, but not MTREC, are essential for *rDNA* integrity

Erh1 also associated with *rDNA* repeats (Figure 6A, top). The binding profile of Erh1 at *rDNA* strikingly resembles that of the RNAi component Ago1 (Figure 6A, bottom), as we described previously (Cam et al., 2005). Given that RNAi is essential for heterochromatin formation and silencing at *rDNA* repeats (Cam et al., 2005), we hypothesized that Erh1 is also involved in the assembly of *rDNA* heterochromatin. As expected, we observed a significant decrease in H3K9me2 at *rDNA* clusters in *erh1*Δ (Figure 6B, top). Considering that we identified MTREC and CCR4-NOT as Erh1-binding partners, we wondered whether Erh1 cooperates with MTREC and/or CCR4-NOT to facilitate heterochromatin assembly at *rDNA*. We found that H3K9me2 levels at *rDNA* repeats were considerably decreased in *ccr4*Δ (Figure 6B, bottom), but were not affected in *red1*Δ (Figure 6C). These results indicate that Erh1 and CCR4-NOT are involved in the assembly of *rDNA* heterochromatin, whereas MTREC is dispensable.

To further confirm heterochromatin loss at *rDNA* repeats, we first examined whether *rDNA* silencing is impaired in *erh1*Δ and *ccr4*Δ. As expected, $ura4^+$ and *LEU2* markers embedded within *rDNA* repeats were de-repressed in *erh1*Δ and *ccr4*Δ (Figure 6D). We next explored whether heterochromatin reduction at *rDNA* clusters in *erh1*Δ and *ccr4*Δ causes increased mitotic recombination at these loci. To assess mitotic recombination, we utilized the *rDNA*::$ura4^+$ marker, which is lost by mitotic recombination when heterochromatin assembly is compromised (Figure 6E, left) (Cam et al., 2005). We observed a marked increase in mitotic recombination at *rDNA* repeats in *erh1*Δ (WT: 2.36×10^{-3}; *erh1*Δ: 2.14×10^{-2}) and in *ccr4*Δ (WT: 2.65×10^{-3}; *ccr4*Δ: 1.46×10^{-2}), as determined by the loss of *rDNA*::$ura4^+$ (Figures 6E, right, S6A and S6B). These results clearly demonstrate that Erh1

and Ccr4 are required to maintain *rDNA* integrity, and indicate that Erh1, CCR4-NOT and RNAi machinery cooperate to establish and/or maintain heterochromatin at *rDNA*.

Subtelomeric heterochromatin is partially affected in *ccr4*Δ

We next investigated whether Ccr4 affects the formation of constitutive heterochromatin. We found that H3K9me2 levels at centromeres and the *mat* locus were unaffected in *ccr4*Δ (Figure S6C). Interestingly, whereas heterochromatin at regions containing *dh*-like elements (within *tlh1*$^+$ and near *SPAC212.06c*) was maintained, we observed considerable decrease in H3K9me2 at subtelomeric domains containing genes upregulated during sexual differentiation and genes encoding transmembrane proteins (Cam et al., 2005; Yamanaka et al., 2013) in *ccr4*Δ (Figures S6D). Consistent with this H3K9me2 reduction, RNA-Seq analysis revealed many upregulated subtelomeric genes in *ccr4*Δ (Figure S6E). Taken together, these data indicate that Ccr4 is required to establish and/or maintain heterochromatin and to repress genes embedded within a specific region at subtelomeres.

Ccr4 plays only a minor role in heterochromatin island assembly, meiotic mRNA decay and meiRNA dot formation

Mmi1 facilitates the assembly of facultative heterochromatin islands via RNAi-independent pathways at many meiotic genes (Hiriart et al., 2012; Tashiro et al., 2013; Zofall et al., 2012). Our finding that Erh1 is essential for the formation of meiotic heterochromatin islands (Figure 5) prompted us to explore whether CCR4-NOT also participates in this process. We found that *ccr4*Δ showed only a slight reduction in H3K9me2 at meiotic islands, with the exception of the *mei4*$^+$ locus (Figure S7A, island 1, 6, 8 and 9), and caused no change at non-meiotic islands (Figure S7A, island 14 and 15). The minor contribution of CCR4-NOT to forming islands other than at the *mei4*$^+$ locus is also supported by a recent report (Cotobal et al., 2015). These observations are in contrast to the complete loss of H3K9me at meiotic islands observed in cells lacking Mmi1, Erh1 or MTREC (Figure 5) (Hiriart et al., 2012; Tashiro et al., 2013; Zofall et al., 2012), and indicates that of the two EMC-associated complexes, MTREC is largely responsible for meiotic heterochromatin islands, whereas CCR4-NOT plays only a minor role.

Although *ccr4*Δ had a minor effect on heterochromatin islands, there was a possibility that, like Erh1, CCR4-NOT mediates degradation of meiotic mRNAs in vegetative cells. We performed RNA-Seq and found that transcripts that accumulated in *erh1*Δ were not significantly increased in *ccr4*Δ (Figures S7B and S7C), and the increase in the Mmi1-regulon (Chen et al., 2011), with the exception of *sme2*, was less than 2 fold in two independent *ccr4*Δ RNA-Seq datasets (Figures S7C). We also examined whether *ccr4*Δ could rescue the sporulation defect of *sme2*Δ, which can be suppressed by mutations that impair meiotic mRNA degradation (Chalamcharla et al., 2015; Harigaya et al., 2006; Sugiyama et al., 2013; Yamashita et al., 2013). However, we observed almost no *sme2*Δ suppression by *ccr4*Δ (Figure S7D), further supporting our conclusion that Ccr4 is dispensable for meiotic mRNA decay in vegetative cells. Moreover, meiRNA dot formation, which depends on Erh1 (Figure 3) and Mmi1 (Shichino et al., 2014), was not considerably affected in the absence of Ccr4 (Figure S7E). We conclude that CCR4-NOT is largely

dispensable for heterochromatin island assembly, meiotic mRNA degradation and meiRNA dot formation.

Loss of Ccr4 affects RNAi-dependent facultative heterochromatin at developmental genes and retrotransposons

HOODs, another class of facultative heterochromatin detected under specific growth conditions or upon deletion of the nuclear exosome subunit Rrp6 (Marasovic et al., 2013; Shah et al., 2014; Yamanaka et al., 2013), coat developmentally and environmentally regulated genes and retrotransposons. HOOD assembly depends on RNAi, and Mmi1 is also required for the formation of some HOODs (Shah et al., 2014; Yamanaka et al., 2013), raising the possibility that Erh1 and CCR4-NOT are also required for HOOD assembly. To test this possibility, we performed H3K9me2 ChIP analyses in *rrp6*Δ, *erh1*Δ *rrp6*Δ and *ccr4*Δ *rrp6*Δ. We found that H3K9me2 at the *mcp3*$^{+}$ locus (*HOOD-12*), which is Mmi1-dependent, was abolished in *erh1*Δ *rrp6*Δ, whereas H3K9me2 at *SPCC1442.04c* (*HOOD-31*) and the *Tf2-5* retrotransposon (*HOOD-10*), both of which are Mmi1-independent, was slightly increased (Figures 7A and S7F). Consistent with this, small RNAs derived from *HOOD-12* were lost whereas small RNAs from *HOOD-31* and *-10* were increased in *erh1*Δ *rrp6*Δ (Figure 7B). Such increases at Mmi1-independent HOODs were also observed in *mmi1*Δ (Yamanaka et al., 2013), indicating that Erh1 and Mmi1 have similar effects on HOOD assembly. Surprisingly, *ccr4*Δ resulted in the loss of H3K9me2 at both EMC-dependent and -independent HOODs (Figures 7A and S7F). Moreover, small RNAs from these HOODs were not detected in *ccr4*Δ *rrp6*Δ (Figure 7B). These results contradict a recent paper reporting that a *ccr4* mutation did not decrease H3K9me2 at HOODs (Cotobal et al., 2015), and indicate that Ccr4 is indeed indispensable for RNAi-dependent H3K9me2 and small RNA generation at HOODs.

Ccr4 cooperates with Pir2/ARS2 to form facultative heterochromatin

To investigate whether CCR4-NOT is linked to factors involved in RNAi, we performed a detailed examination of results from biochemical purifications including mass spectrometry analyses of various RNA elimination factors. These analyses led to an unexpected observation that all seven subunits of CCR4-NOT co-purified with an evolutionarily conserved protein, Pir2/Ars2, which also associates with MTREC and the Cap-binding complex (CBC) (Egan et al., 2014; Lee et al., 2013; Zhou et al., 2015). We confirmed that Pir2-FLAG co-immunoprecipitates with Ccr4-GFP (Figure 7C). Intriguingly, ARS2 is involved in RNAi in *Drosophila* and *Arabidopsis* (Sabin et al., 2009; Yang et al., 2006), which suggested a potential biological significance for the CCR4-NOT-Pir2 interaction.

We isolated a temperature-sensitive loss of function *pir2* allele (*pir2-1*), since *pir2*$^{+}$ is essential for cell viability (Kim et al., 2010). The *pir2-1* mutant contained two amino acid substitutions: F165L in the DUF3546 domain, whose function is unknown, and S316P between the DUF3546 and ARS2 domains (Figure 7D, top). The *pir2-1* strain grew slower than WT at 26°C and 33°C, and did not grow at 36°C (Figure 7D, bottom). The *pir2-1* mutant showed a reduction in H3K9me2 and silencing at centromeres (G.T., J.D. and S.I.S.G., unpublished data). Remarkably, we also found that Pir2 affects RNAi-mediated heterochromatin assembly at both EMC-dependent and -independent HOODs, in a manner

similar to CCR4-NOT. H3K9me2 levels at both EMC-dependent and -independent HOODs were reduced in *rrp6Δ pir2-1* (Figure 7E). Moreover, our Northern blot analysis showed that small RNA generation at these HOODs was also severely impaired (Figure 7F). These results clearly show that CCR4-NOT works with Pir2/ARS2 for the assembly of facultative heterochromatin at retrotransposons as well as at developmentally regulated genes.

DISCUSSION

Here we identify Mmi1 as a binding partner of Erh1, and demonstrate that EMC cooperates with conserved RNA processing factors to promote meiotic mRNA degradation and facultative heterochromatin assembly. In addition to engaging MTREC for mRNA decay and assembly of heterochromatin islands at meiotic genes, EMC also interacts with CCR4-NOT to promote the formation of RNAi-dependent heterochromatin domains at developmental genes, retrotransposons and *rDNA*. However, unlike EMC and MTREC, CCR4-NOT plays only a minor role in silencing meiotic genes and forming heterochromatin islands in vegetative cells. Thus, it appears that EMC connects with distinct factors to perform different functions. Our results provide insights into the functions of Erh1 and its associated factors in the regulation of gene expression and the maintenance of genome stability.

EMC, a complex involved in meiotic mRNA decay

Although functionally connected, EMC and MTREC comprise distinct complexes based on the following observations: (1) Erh1 purification identified Mmi1 as a stoichiometric binding partner, but recovered a relatively low amount of MTREC subunits; (2) the localization of Erh1 and Red1 is not mutually dependent; (3) Erh1, but not Red1, is required for Mei2-meiRNA dot formation and for maintenance of *rDNA* integrity; and (4) previous purification studies did not indicate that Red1 interacts with Erh1 (Egan et al., 2014; Lee et al., 2013; Zhou et al., 2015). Therefore, we propose that EMC, like MTREC and the nuclear exosome, is another complex essential for meiotic mRNA degradation, and that these complexes cooperate to degrade meiotic mRNAs.

Mmi1 is essential for viability and temperature-sensitive *mmi1* mutants cannot be used to study meiosis because high temperatures inhibit meiosis (Sabatinos and Forsburg, 2010). Thus, the fact that the *erh1*Δ strain is viable and does sporulate makes it a particularly useful tool to study EMC functions in meiosis such as meiRNA formation and homologous chromosome pairing (Ding et al., 2012; Shichino et al., 2014). Moreover, these results indicate that Mmi1 likely has additional functions independent of Erh1, either in meiotic mRNA elimination or other biological processes.

The possible function of Erh1 in EMC

The proteins of the ERH family are small (~12 kDa) and have reported roles in different kinds of nuclear transactions, including transcriptional repression, transcriptional elongation, mRNA splicing and translation (Weng and Luo, 2013). These observations suggest that ERH modulates the function(s) of its binding partners, rather than suggesting ERH has multiple activities. Given that mammalian ERH forms homodimers in solution (Arai et al.,

2005; Wan et al., 2005), it is possible that Erh1 mediates Mmi1 dimerization, thereby allowing Mmi1 to exert its RNA-binding activity *in vivo*. Indeed, dimerization is known to be a prerequisite for the function of STAR, which is a subfamily of KH domain-containing RNA-binding proteins (Feracci et al., 2014), and hnRNP C forms tetramers to measure RNA length (McCloskey et al., 2012).

Another not mutually exclusive possibility is that the Mmi1 nuclear foci, which depend on Erh1, are required for Mmi1 function. Although we previously suggested that the formation of Red1 foci may correlate with mRNA degradation activity (Sugiyama and Sugioka-Sugiyama, 2011), it remains unclear whether the assembly of nuclear bodies by RNA elimination factors is required for mRNA degradation, and whether they are the place where RNA degradation occurs. Further analyses, such as the isolation of mutants that affect the localization of RNA elimination factors, may reveal the biological significance of nuclear body formation.

Erh1, CCR4-NOT and Pir2/ARS2: additional factors involved in H3K9 methylation

Our analyses also revealed that Erh1 is required for heterochromatin formation at meiotic genes. Moreover, defects in CCR4-NOT affect heterochromatin distribution at *rDNA*, HOODs and subtelomeres. At subtelomeric regions, heterochromatin consists of two distinct domains: *dh*-like sequences and the adjacent regions that contain meiosis-upregulated genes and transmembrane protein genes (Cam et al., 2005; Yamanaka et al., 2013). Impaired H3K9me2 in *ccr4*Δ is largely restricted to the latter region. Since RNA elimination factors (Sugiyama and Sugioka-Sugiyama, 2011; Yamanaka et al., 2013) and Ccr4 (this study) control the expression of genes embedded within these regions at subtelomeres, it is conceivable that CCR4-NOT directly participates in this process through the assembly of heterochromatin domains coating these loci. These heterochromatin domains located adjacent to blocks of telomeric heterochromatin resemble HOODs that also require CCR4-NOT and RNA elimination factors for small RNA production and H3K9 methylation.

Independently of our study, CCR4-NOT function in H3K9me was recently reported (Cotobal et al., 2015). Although both studies show the role of CCR4-NOT in H3K9me, there are profound differences in our conclusions. First, we demonstrate that CCR4-NOT is required for *rDNA* heterochromatin and *rDNA* integrity, a finding that was not reported by Cotobal et al., (Cotobal et al., 2015). Second, we show that CCR4-NOT is a critical player for H3K9 methylation and small RNA generation at HOODs, whereas Cotobal and colleagues reported that *ccr4* and *caf1* mutations do not affect HOODs (Cotobal et al., 2015). Third, we find that *ccr4*Δ has only a minor impact on Red1-dependent heterochromatin islands, with the exception of island 9 (the *mei4*$^{+}$ locus). Although these results are in agreement with the data recently reported by Cotobal et al., (2015), the authors claimed that CCR4-NOT is essential for Mmi1-dependent islands (Cotobal et al., 2015). Based on our current and previous results (Lee et al., 2013; Yamanaka et al., 2013; Zofall et al., 2012), we propose that: (1) EMC and MTREC are the major players in heterochromatin island assembly, and (2) CCR4-NOT facilitates heterochromatin assembly at *rDNA* repeats, subtelomeres, and HOODs (Figure 7G).

We find that Ccr4 and Pir2/ARS2, both of which interact with each other, play an essential role in HOOD assembly, and that Pab2 also co-purifies with Ccr4. As HOOD assembly depends on RNAi, Pab2, cryptic introns and splicing factors (Lee et al., 2013; Yamanaka et al., 2013), it is plausible that CCR4-NOT and Pir2 are recruited by splicing factors (and EMC at certain loci) and cooperate with RNAi to assemble HOODs. Supporting this idea, it has been shown that: (1) ARS2 interacts with Dicer in *Drosophila* and *Arabidopsis* and is involved in RNAi (Sabin et al., 2009; Yang et al., 2006); (2) *C. elegans ntl-9*, a subunit of CCR4-NOT, is required to generate siRNAs from its endogenous targets (Fischer et al., 2013); and (3) human ARS2 co-purifies with the spliceosome (Rappsilber et al., 2002). Alternatively, Pir2 may facilitate HOOD assembly through non-canonical transcription termination. This idea is based on the following studies: (1) ARS2 has been shown to promote transcription termination (Andersen et al., 2013; Gruber et al., 2012; Hallais et al., 2013); and (2) Dhp1/Xrn2, a transcription termination factor, plays an essential role in HOOD assembly (Chalamcharla et al., 2015).

Perspective

Our findings are likely to have important biological implications. Heterochromatin formation at HOODs is controlled by growth conditions and developmental signals (Yamanaka et al., 2013). Since the functions of CCR4-NOT can be modulated by environmental and developmental cues (Miller and Reese, 2012), this machinery may facilitate cellular adaptation to different growth conditions. Furthermore, inappropriate expression of germline/meiosis-specific genes in somatic cells can induce tumor formation. In *Drosophila*, mutations in *lethal (3) malignant brain tumor* [*l(3)mbt*] are associated with brain tumors and are accompanied by ectopic expression of germline genes including *piwi*, *aub* and *nos*. Mutation of *piwi*, *aub* or *nos* is sufficient to suppress the brain tumor caused by *l(3)mbt* (Janic et al., 2010), indicating that Piwi, Aub or Nos plays a direct role in tumorigenesis. In recent years, much interest is focused on the identification of tumor-specific antigens, which can provide potential targets for immunotherapy. The continuing search for human tumor-specific antigens has identified more than 40 genes that are normally expressed in gametes. Called C/T (cancer/testis) antigens, their abnormal expression in somatic cells is suspected to induce genomic instability (Simpson et al., 2005; Whitehurst, 2014). Therefore, it has become clinically relevant to uncover the mechanism(s) by which aberrant expression of germline-specific genes is suppressed in somatic cells. It would be of great biological and clinical interest to test whether conserved RNA processing factors contribute to suppression of C/T antigen expression in somatic cells of higher eukaryotes.

EXPERIMENTAL PROCEDURES

Yeast strain construction and cell culture were performed using standard methods (Moreno et al., 1991). The *pir2-1* mutant was constructed using an error-prone PCR-based method as described previously (Lee et al., 2013; Sugiyama et al., 2013). Strains and primers used in this study are listed in Tables S6 and S7, respectively. Dilution analyses, mating efficiency assays, and *rDNA*::*ura4*$^{+}$ loss assays were performed as described previously (Cam et al., 2005; Sugiyama and Sugioka-Sugiyama, 2011). Briefly, for the *rDNA*::*ura4*$^{+}$ loss assay,

strains carrying *LEU2* and *ura4*$^+$ reporter genes inserted at tandem *rDNA* repeats were plated on medium lacking leucine, propagated in non-selective liquid YEA and plated on YEA medium plates followed by replica plating onto medium lacking uracil (-Ura). Cells that grew on YEA but not on -Ura were counted as *ura4*$^+$ loss clones. Loss of *ura4*$^+$ was confirmed by PCR using Terra™ PCR Direct Polymerase Mix (TaKaRa Bio). A DeltaVision Elite (Applied Precision, GE Healthcare) was used for differential interference contrast and fluorescence microscopy. The raw images were captured and analyzed using softWoRx (Applied Precision, GE Healthcare). RNA sequencing, Northern blotting, Western blotting, ChIP, ChIP-chip, protein purification and mass spectrometry analyses were performed as described previously (Cam et al., 2005; Lee et al., 2013; Sugiyama et al., 2007). Detailed procedures and associated references are available in the Supplemental Experimental Procedures.

Supplementary Material

Refer to Web version on PubMed Central for supplementary material.

ACKNOWLEDGEMENT

We thank J. Cooper, A. Kelly, K. Sawin, K. Tatebayashi, Y. Watanabe, M. Yamamoto, A. Yamashita and the National Bio Resource Project (NBRP) of the MEXT, Japan for *S. pombe* strains and materials; H. P. Cam, H. D. Folco, S. Yamanaka and M. Zofall for technical advice; J. Barrowman for her valuable help in editing the manuscript; and members of the Grewal lab for helpful discussions. T.S. thanks R. Sugioka-Sugiyama for her support. This research was supported by the intramural Research Program of the National Institutes of Health and by the National Cancer Institute.

REFERENCES

Andersen PR, Domanski M, Kristiansen MS, Storvall H, Ntini E, Verheggen C, Schein A, Bunkenborg J, Poser I, Hallais M, et al. The human cap-binding complex is functionally connected to the nuclear RNA exosome. Nat. Struct. Mol. Biol. 2013; 20:1367–1376. [PubMed: 24270879]

Arai R, Kukimoto-Niino M, Uda-Tochio H, Morita S, Uchikubo-Kamo T, Akasaka R, Etou Y, Hayashizaki Y, Kigawa T, Terada T, et al. Crystal structure of an enhancer of rudimentary homolog (ERH) at 2.1 Angstroms resolution. Protein Sci. 2005; 14:1888–1893. [PubMed: 15937287]

Ard R, Tong P, Allshire RC. Long non-coding RNA-mediated transcriptional interference of a permease gene confers drug tolerance in fission yeast. Nat. Commun. 2014; 5:5576. [PubMed: 25428589]

Cam HP, Sugiyama T, Chen ES, Chen X, FitzGerald PC, Grewal SI. Comprehensive analysis of heterochromatin- and RNAi-mediated epigenetic control of the fission yeast genome. Nat. Genet. 2005; 37:809–819. [PubMed: 15976807]

Chalamcharla VR, Folco HD, Dhakshnamoorthy J, Grewal SI. Conserved factor Dhp1/Rat1/Xrn2 triggers premature transcription termination and nucleates heterochromatin to promote gene silencing. Proc. Natl. Acad. Sci. USA. 2015; 112:15548–15555. [PubMed: 26631744]

Chen HM, Futcher B, Leatherwood J. The fission yeast RNA binding protein Mmi1 regulates meiotic genes by controlling intron specific splicing and polyadenylation coupled RNA turnover. PloS One. 2011; 6:e26804. [PubMed: 22046364]

Cotobal C, Rodriguez-Lopez M, Duncan C, Hasan A, Yamashita A, Yamamoto M, Bahler J, Mata J. Role of Ccr4-Not complex in heterochromatin formation at meiotic genes and subtelomeres in fission yeast. Epigenet. Chromatin. 2015; 8:28.

Ding DQ, Okamasa K, Yamane M, Tsutsumi C, Haraguchi T, Yamamoto M, Hiraoka Y. Meiosis-specific noncoding RNA mediates robust pairing of homologous chromosomes in meiosis. Science. 2012; 336:732–736. [PubMed: 22582262]

Egan ED, Braun CR, Gygi SP, Moazed D. Post-transcriptional regulation of meiotic genes by a nuclear RNA silencing complex. RNA. 2014; 20:867–881. [PubMed: 24713849]

Feracci M, Foot J, Dominguez C. Structural investigations of the RNA-binding properties of STAR proteins. Biochem. Soc. Trans. 2014; 42:1141–1146. [PubMed: 25110016]

Fischer SE, Pan Q, Breen PC, Qi Y, Shi Z, Zhang C, Ruvkun G. Multiple small RNA pathways regulate the silencing of repeated and foreign genes in *C. elegans*. Genes Dev. 2013; 27:2678–2695. [PubMed: 24352423]

Gruber JJ, Olejniczak SH, Yong J, La Rocca G, Dreyfuss G, Thompson CB. Ars2 promotes proper replication-dependent histone mRNA 3′ end formation. Mol. Cell. 2012; 45:87–98. [PubMed: 22244333]

Hallais M, Pontvianne F, Andersen PR, Clerici M, Lener D, Benbahouche Nel H, Gostan T, Vandermoere F, Robert MC, Cusack S, et al. CBC-ARS2 stimulates 3′-end maturation of multiple RNA families and favors cap-proximal processing. Nat. Struct. Mol. Biol. 2013; 20:1358–1366. [PubMed: 24270878]

Harigaya Y, Tanaka H, Yamanaka S, Tanaka K, Watanabe Y, Tsutsumi C, Chikashige Y, Hiraoka Y, Yamashita A, Yamamoto M. Selective elimination of messenger RNA prevents an incidence of untimely meiosis. Nature. 2006; 442:45–50. [PubMed: 16823445]

Harigaya Y, Yamashita A, Tanaka K, Yamamoto M. [Selective elimination of meiosis-specific mRNA operates during the mitotic cell cycle]. Tanpakushitsu Kakusan Koso. 2007; 52:1–10. [PubMed: 17228834]

Hiriart E, Vavasseur A, Touat-Todeschini L, Yamashita A, Gilquin B, Lambert E, Perot J, Shichino Y, Nazaret N, Boyault C, et al. Mmi1 RNA surveillance machinery directs RNAi complex RITS to specific meiotic genes in fission yeast. EMBO J. 2012; 31:2296–2308. [PubMed: 22522705]

Janic A, Mendizabal L, Llamazares S, Rossell D, Gonzalez C. Ectopic expression of germline genes drives malignant brain tumor growth in *Drosophila*. Science. 2010; 330:1824–1827. [PubMed: 21205669]

Kim DU, Hayles J, Kim D, Wood V, Park HO, Won M, Yoo HS, Duhig T, Nam M, Palmer G, et al. Analysis of a genome-wide set of gene deletions in the fission yeast *Schizosaccharomyces pombe*. Nat. Biotechnol. 2010; 28:617–623. [PubMed: 20473289]

Krzyzanowski MK, Kozlowska E, Kozlowski P. Identification and functional analysis of the *erh1*$^{+}$ gene encoding enhancer of rudimentary homolog from the fission yeast *Schizosaccharomyces pombe*. PloS One. 2012; 7:e49059. [PubMed: 23145069]

Lee NN, Chalamcharla VR, Reyes-Turcu F, Mehta S, Zofall M, Balachandran V, Dhakshnamoorthy J, Taneja N, Yamanaka S, Zhou M, et al. Mtr4-like protein coordinates nuclear RNA processing for heterochromatin assembly and for telomere maintenance. Cell. 2013; 155:1061–1074. [PubMed: 24210919]

Marasovic M, Zocco M, Halic M. Argonaute and Triman generate dicer-independent priRNAs and mature siRNAs to initiate heterochromatin formation. Mol. Cell. 2013; 52:173–183. [PubMed: 24095277]

Mata J, Lyne R, Burns G, Bahler J. The transcriptional program of meiosis and sporulation in fission yeast. Nat. Genet. 2002; 32:143–147. [PubMed: 12161753]

McCloskey A, Taniguchi I, Shinmyozu K, Ohno M. hnRNP C tetramer measures RNA length to classify RNA polymerase II transcripts for export. Science. 2012; 335:1643–1646. [PubMed: 22461616]

Miller JE, Reese JC. Ccr4-Not complex: the control freak of eukaryotic cells. Criti. Rev. Biochem. Mol. Biol. 2012; 47:315–333.

Moreno S, Klar A, Nurse P. Molecular genetic analysis of fission yeast *Schizosaccharomyces pombe*. Methods Enzymol. 1991; 194:795–823. [PubMed: 2005825]

Rappsilber J, Ryder U, Lamond AI, Mann M. Large-scale proteomic analysis of the human spliceosome. Genome Res. 2002; 12:1231–1245. [PubMed: 12176931]

Sabatinos SA, Forsburg SL. Molecular genetics of *Schizosaccharomyces pombe*. Methods Enzymol. 2010; 470:759–795. [PubMed: 20946835]

Sabin LR, Zhou R, Gruber JJ, Lukinova N, Bambina S, Berman A, Lau CK, Thompson CB, Cherry S. Ars2 regulates both miRNA- and siRNA-dependent silencing and suppresses RNA virus infection in *Drosophila*. Cell. 2009; 138:340–351. [PubMed: 19632183]

Shah S, Wittmann S, Kilchert C, Vasiljeva L. lncRNA recruits RNAi and the exosome to dynamically regulate *pho1* expression in response to phosphate levels in fission yeast. Genes Dev. 2014; 28:231–244. [PubMed: 24493644]

Shichino Y, Yamashita A, Yamamoto M. Meiotic long non-coding meiRNA accumulates as a dot at its genetic locus facilitated by Mmi1 and plays as a decoy to lure Mmi1. Open Biol. 2014; 4:140022. [PubMed: 24920274]

Simpson AJ, Caballero OL, Jungbluth A, Chen YT, Old LJ. Cancer/testis antigens, gametogenesis and cancer. Nat. Rev. Cancer. 2005; 5:615–625. [PubMed: 16034368]

St-Andre O, Lemieux C, Perreault A, Lackner DH, Bahler J, Bachand F. Negative regulation of meiotic gene expression by the nuclear poly(a)-binding protein in fission yeast. J. Biol. Chem. 2010; 285:27859–27868. [PubMed: 20622014]

Sugiyama T, Cam HP, Sugiyama R, Noma K, Zofall M, Kobayashi R, Grewal SI. SHREC, an effector complex for heterochromatic transcriptional silencing. Cell. 2007; 128:491–504. [PubMed: 17289569]

Sugiyama T, Sugioka-Sugiyama R. Red1 promotes the elimination of meiosis-specific mRNAs in vegetatively growing fission yeast. EMBO J. 2011; 30:1027–1039. [PubMed: 21317872]

Sugiyama T, Wanatabe N, Kitahata E, Tani T, Sugioka-Sugiyama R. Red5 and three nuclear pore components are essential for efficient suppression of specific mRNAs during vegetative growth of fission yeast. Nucleic Acids Res. 2013; 41:6674–6686. [PubMed: 23658229]

Tashiro S, Asano T, Kanoh J, Ishikawa F. Transcription-induced chromatin association of RNA surveillance factors mediates facultative heterochromatin formation in fission yeast. Genes Cells. 2013; 18:327–339. [PubMed: 23388053]

Wan C, Tempel W, Liu ZJ, Wang BC, Rose RB. Structure of the conserved transcriptional repressor enhancer of rudimentary homolog. Biochemistry. 2005; 44:5017–5023. [PubMed: 15794639]

Weng MT, Luo J. The enigmatic ERH protein: its role in cell cycle, RNA splicing and cancer. Protein Cell. 2013; 4:807–812. [PubMed: 24078386]

Whitehurst AW. Cause and consequence of cancer/testis antigen activation in cancer. Annu. Rev. Pharmacol. Toxicol. 2014; 54:251–272. [PubMed: 24160706]

Wilhelm BT, Marguerat S, Watt S, Schubert F, Wood V, Goodhead I, Penkett CJ, Rogers J, Bahler J. Dynamic repertoire of a eukaryotic transcriptome surveyed at single-nucleotide resolution. Nature. 2008; 453:1239–1243. [PubMed: 18488015]

Wojcik E, Murphy AM, Fares H, Dang-Vu K, Tsubota SI. *Enhancer of rudimentary*^{p1}, *e(r)*^{p1}, a highly conserved enhancer of the *rudimentary* gene. Genetics. 1994; 138:1163–1170. [PubMed: 7896098]

Yamamoto M. The molecular control mechanisms of meiosis in fission yeast. Trends Biochem. Sci. 1996a; 21:18–22. [PubMed: 8848833]

Yamamoto M. Regulation of meiosis in fission yeast. Cell Struct. Funct. 1996b; 21:431–436. [PubMed: 9118252]

Yamanaka S, Mehta S, Reyes-Turcu FE, Zhuang F, Fuchs RT, Rong Y, Robb GB, Grewal SI. RNAi triggered by specialized machinery silences developmental genes and retrotransposons. Nature. 2013; 493:557–560. [PubMed: 23151475]

Yamanaka S, Yamashita A, Harigaya Y, Iwata R, Yamamoto M. Importance of polyadenylation in the selective elimination of meiotic mRNAs in growing *S. pombe* cells. EMBO J. 2010; 29:2173–2181. [PubMed: 20512112]

Yamashita A, Shichino Y, Tanaka H, Hiriart E, Touat-Todeschini L, Vavasseur A, Ding DQ, Hiraoka Y, Verdel A, Yamamoto M. Hexanucleotide motifs mediate recruitment of the RNA elimination machinery to silent meiotic genes. Open Biol. 2012; 2:120014. [PubMed: 22645662]

Yamashita A, Takayama T, Iwata R, Yamamoto M. A novel factor Iss10 regulates Mmi1-mediated selective elimination of meiotic transcripts. Nucleic Acids Res. 2013; 41:9680–9687. [PubMed: 23980030]

Yang L, Liu Z, Lu F, Dong A, Huang H. SERRATE is a novel nuclear regulator in primary microRNA processing in *Arabidopsis*. Plant J. 2006; 47:841–850. [PubMed: 16889646]

Zhou Y, Zhu J, Schermann G, Ohle C, Bendrin K, Sugioka-Sugiyama R, Sugiyama T, Fischer T. The fission yeast MTREC complex targets CUTs and unspliced pre-mRNAs to the nuclear exosome. Nat. Commun. 2015; 6:7050. [PubMed: 25989903]

Zofall M, Yamanaka S, Reyes-Turcu FE, Zhang K, Rubin C, Grewal SI. RNA elimination machinery targeting meiotic mRNAs promotes facultative heterochromatin formation. Science. 2012; 335:96–100. [PubMed: 22144463]

Highlights

- Erh1 stoichiometrically interacts with Mmi1 to form a complex called EMC
- EMC engages MTREC and CCR4-NOT to assemble facultative heterochromatin
- Ccr4 cooperates with Pir2/ARS2 to trigger RNAi-mediated facultative heterochromatin
- Erh1 and CCR4-NOT promote *rDNA* silencing and the maintenance of *rDNA* integrity

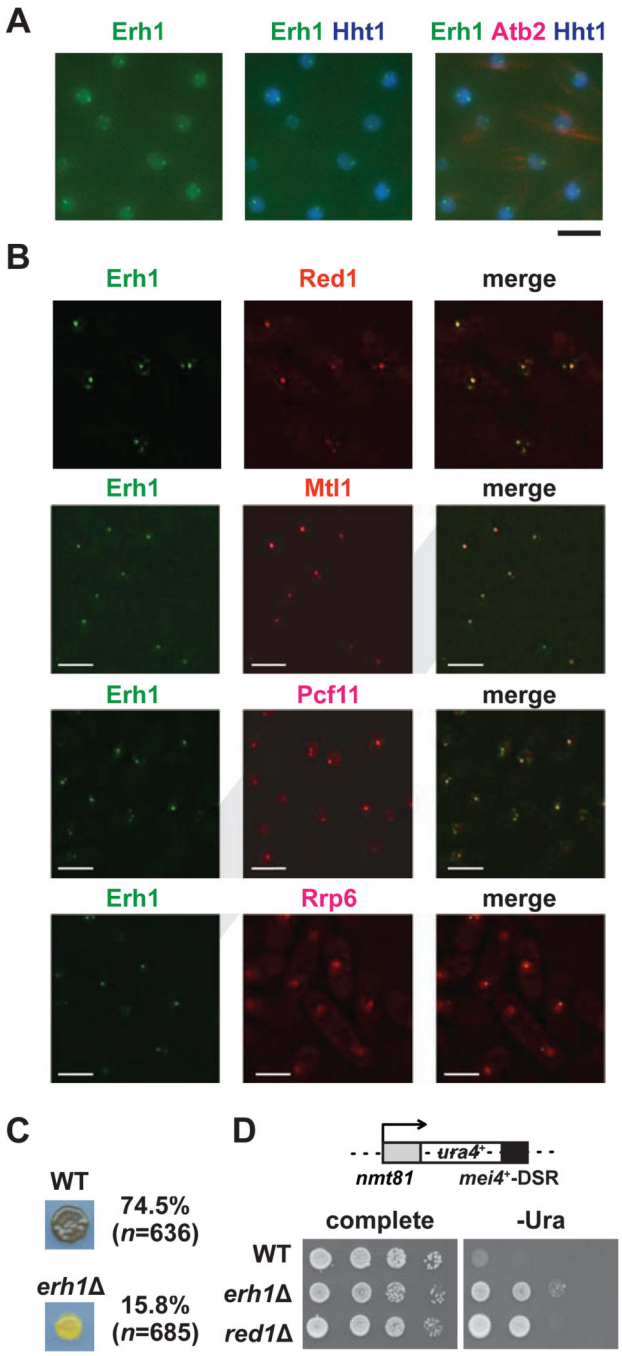

Figure 1. Characterization of Erh1

(A) Erh1 forms nuclear foci. Representative images of vegetative fission yeast cells expressing Erh1-GFP (Erh1), Hht1 (histone H3 h3.1)-CFP and mCherry-Atb2 (tubulin alpha2; used to confirm mitotic interphase) are shown. Bar, 5 μm. (B) Erh1 colocalizes with Red1, Mtl1, Pcf11 and Rrp6. Deconvolved images of vegetative fission yeast cells expressing Erh1-GFP (Erh1) with either Red1-tdTomato (Red1), Mtl1-tdTomato (Mtl1), Pcf11-mCherry (Pcf11) or Rrp6-mCherry (Rrp6) are shown. Bars, 5 μm. (C) Cells from a parental WT or *erh1*Δ homothallic culture were spotted onto minimal (PMG) plates and

incubated at 26°C for 3 days. The presence or absence of asci was determined by iodine staining, and the mating efficiencies are noted; "*n*" indicates the number of cells counted in each strain. (D) Erh1 is required for DSR-dependent mRNA decay. The *ura4*$^{+}$-DSR construct is shown (top). WT, *erh1*Δ, and *red1*Δ cells carrying the *ura4*$^{+}$-DSR were spotted onto complete or uracil-lacking (-ura) minimal plates in the absence of thiamine and then were incubated at 30°C for 3 days (bottom). See also Figure S1.

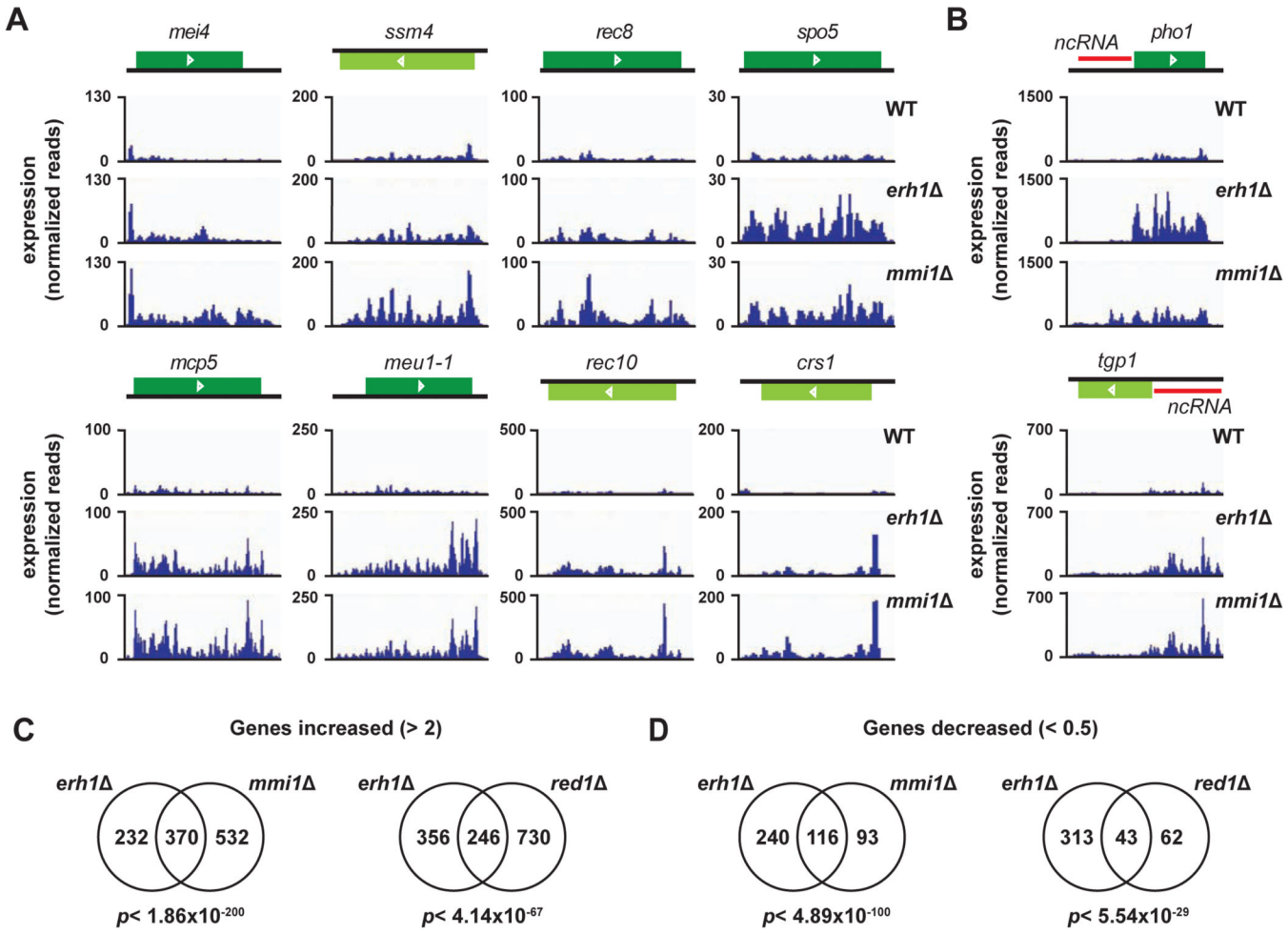

Figure 2. Erh1 shares target transcripts with Mmi1 and Red1

(A) DSR-containing meiotic mRNA levels in *erh1*Δ and *mmi1*Δ. RNA-Seq data of 8 representative meiotic mRNAs in WT, *erh1*Δ and *mmi1*Δ are shown. (B) Expression levels of *pho1*$^{+}$ and *tgp1*$^{+}$. Red bars indicate non-coding RNAs. (C and D) The numbers of genes with increased >2-fold (C) or decreased <0.5-fold (D) expression levels in *erh1*Δ, *mmi1*Δ or *red1*Δ cells are presented in Venn diagrams. For each comparison, the same set of 7019 genes was examined. The statistical significance (*p*-value) of the overlap between each of the two groups is shown under the diagrams. See also Figure S2; Tables S1 and S2.

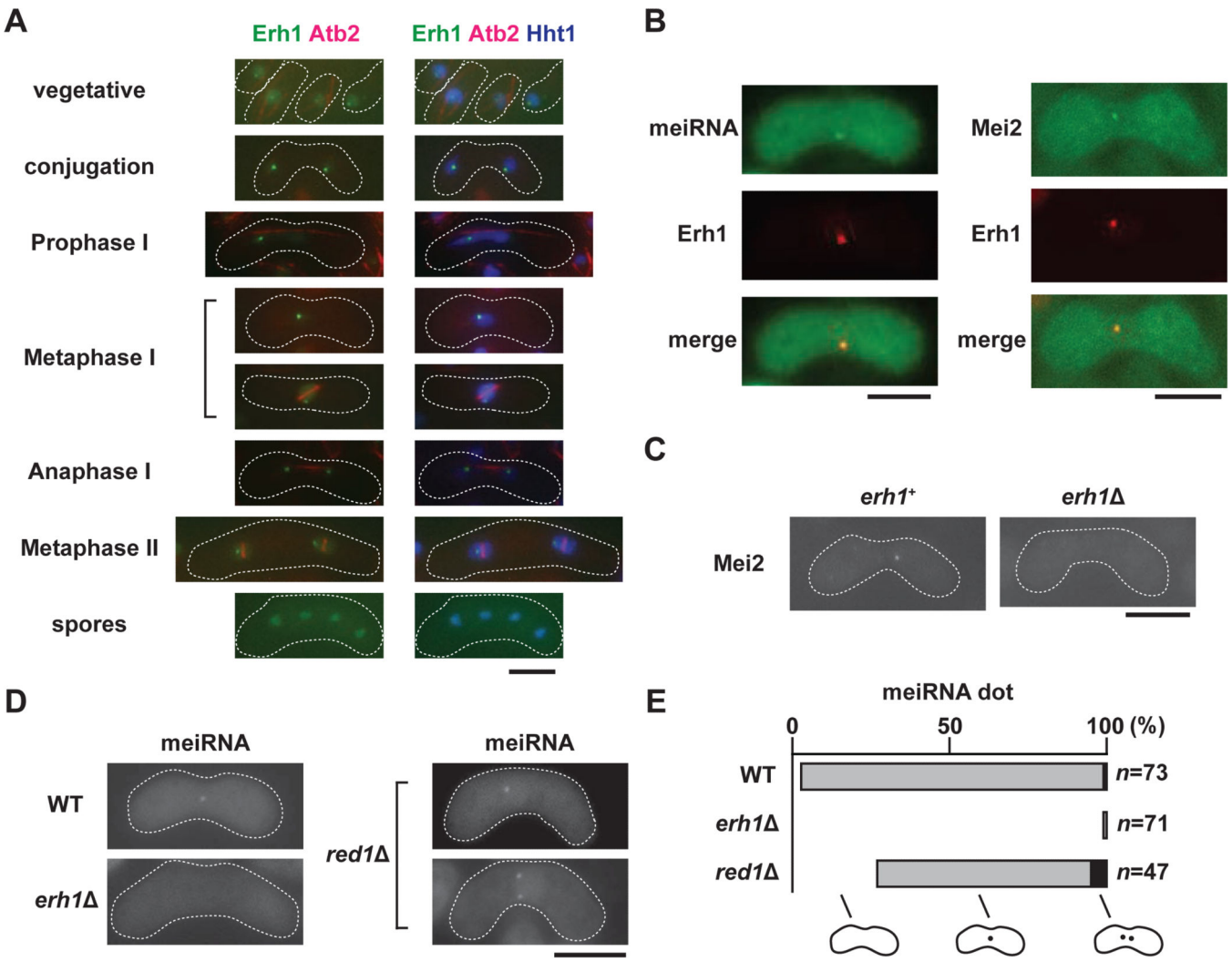

Figure 3. Erh1 localization and function in meiotic cells

(A) Localization of Erh1 during meiosis. Meiosis was induced in homothallic cells expressing Erh1-GFP, mCherry-Atb2 and Hht1-CFP, and the localization of these fluorescent proteins was determined. (B) Erh1 colocalizes with Mei2 and the meiRNA dot. Homothallic strains expressing Erh1-mCherry (Erh1) with either meiRNA, which was visualized using the MS2-loop and MS2-GFP system, or Mei2-GFP were spotted onto minimal (PMG) plates and then incubated at 26°C for 1-2 days to induce meiosis prior to imaging. (C) The Mei2 focus disappears in *erh1*Δ. The localization of Mei2-GFP in meiotic WT and *erh1*Δ cells is shown. (D) Erh1 is essential for meiRNA dot formation. The meiRNA dot in meiotic WT, *erh1*Δ, and *red1*Δ cells was visualized by the MS2-loop and MS2-GFP system. (E) The percentages of cells with 0 (white), 1 (grey) or 2 (black) meiRNA dots are shown in the bar graph. "*n*" indicates the number of cells examined for each strain. Representative images are shown, and the white dashed lines indicate the cell shape. Bars, 5 μm. See also Figure S3.

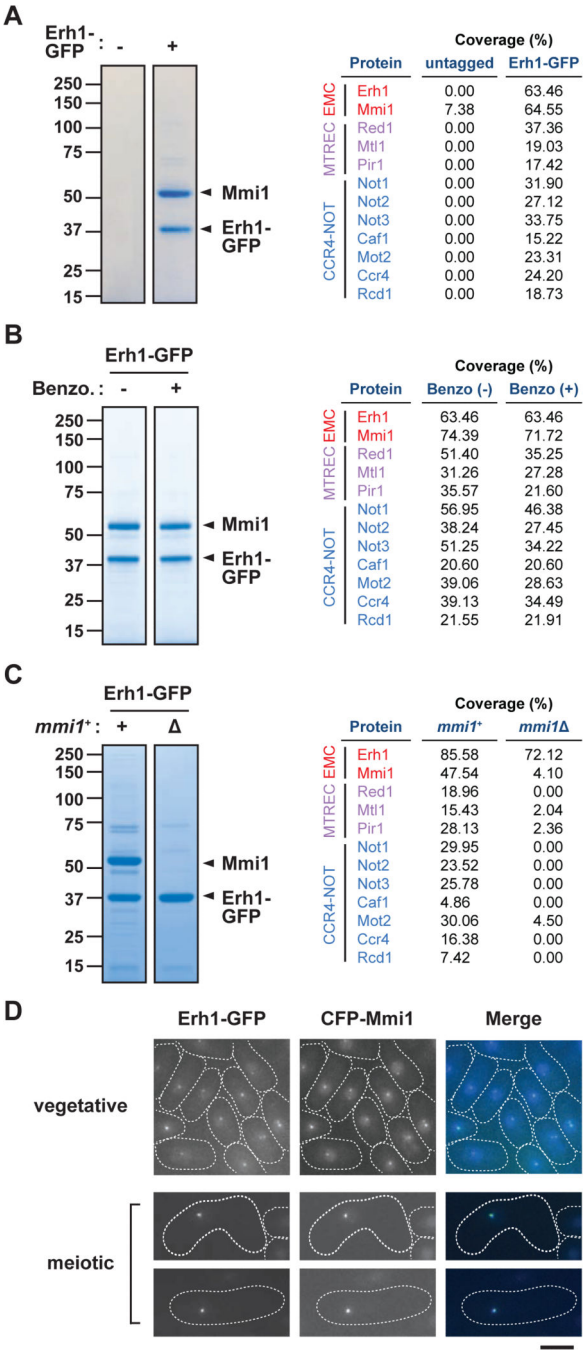

Figure 4. Erh1 forms a complex with the YTH domain containing protein Mmi1

(A) Erh1 purification. Extracts from the parental (untagged) or Erh1-GFP strains were purified on anti-GFP agarose. Erh1-binding proteins were visualized on an SDS-PAGE gel by CBB staining (left). The total peptide coverage (%) of the identified proteins is shown (right). (B) Erh1 purification with or without Benzonase treatment. The extract from the Erh1-GFP strain was purified on anti-GFP agarose with (+) or without (−) Benzonase treatment. The purified fractions were analyzed on an SDS-PAGE gel followed by CBB staining (left). The total peptide coverage (%) of the identified proteins is shown (right). (C)

Erh1 purification from *mmi1*Δ cells. Extracts from WT (+) or *mmi1*Δ (Δ) strains expressing Erh1-GFP were subjected to affinity-purification using anti-GFP agarose. Purified proteins were resolved by SDS-PAGE and visualized by CBB staining (left). The total peptide coverage (%) of the identified proteins is shown (right). (D) Erh1 colocalizes with Mmi1. Representative images of vegetative or meiotic cells expressing Erh1-GFP and CFP-Mmi1 are shown. Bar, 5μm. See also Figure S4 and Tables S3-S5.

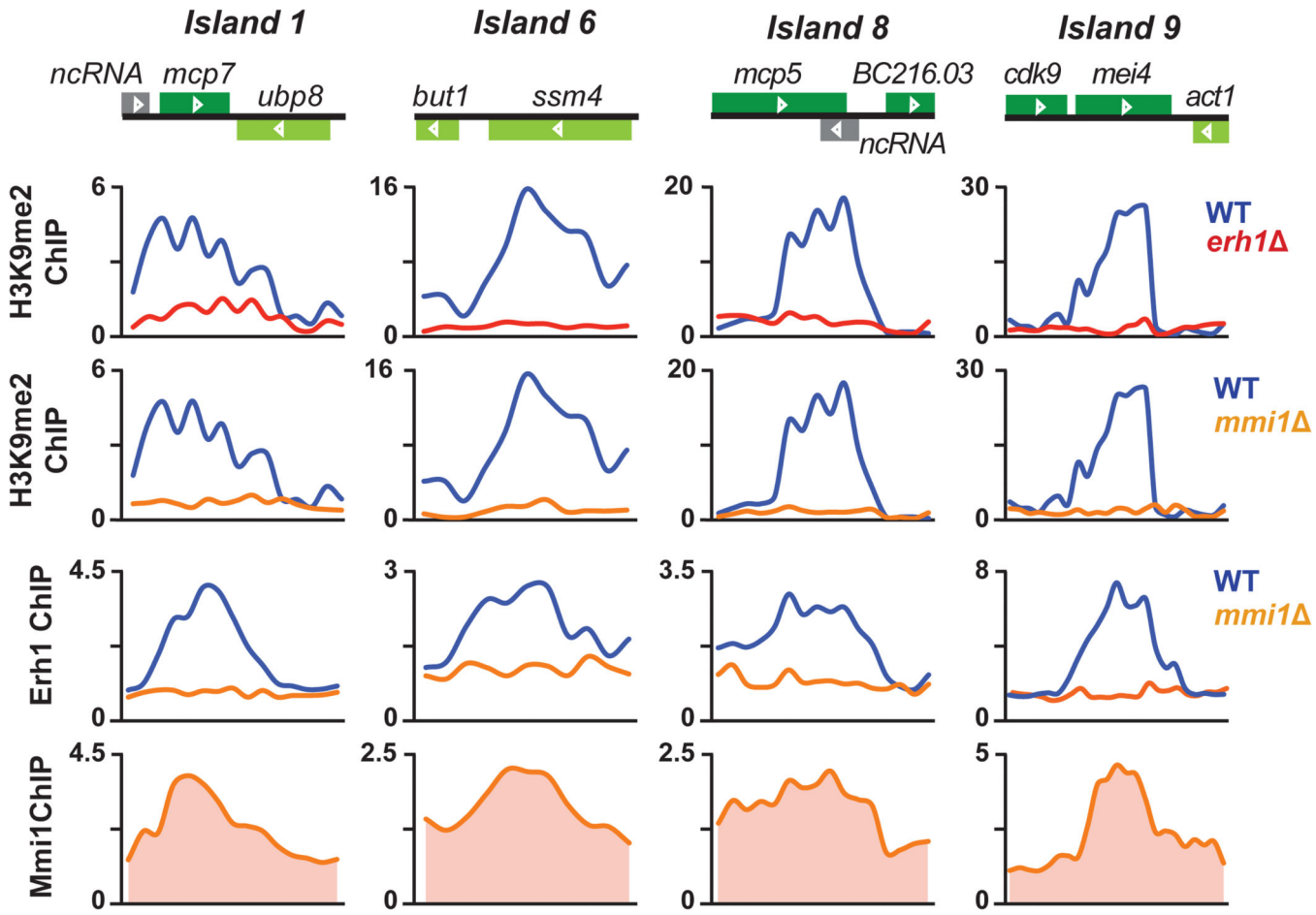

Figure 5. EMC is required for the assembly of heterochromatin islands

ChIP-chip of H3K9me2 at Red1-dependent (1, 6, 8 and 9) islands in WT and *erh1*Δ, and in WT and *mmi1*Δ is shown in the top panels. ChIP-chip of Erh1-GFP in WT and *mmi1*Δ, and of CFP-Mmi1 in WT is shown in the bottom panels. See also Figure S5.

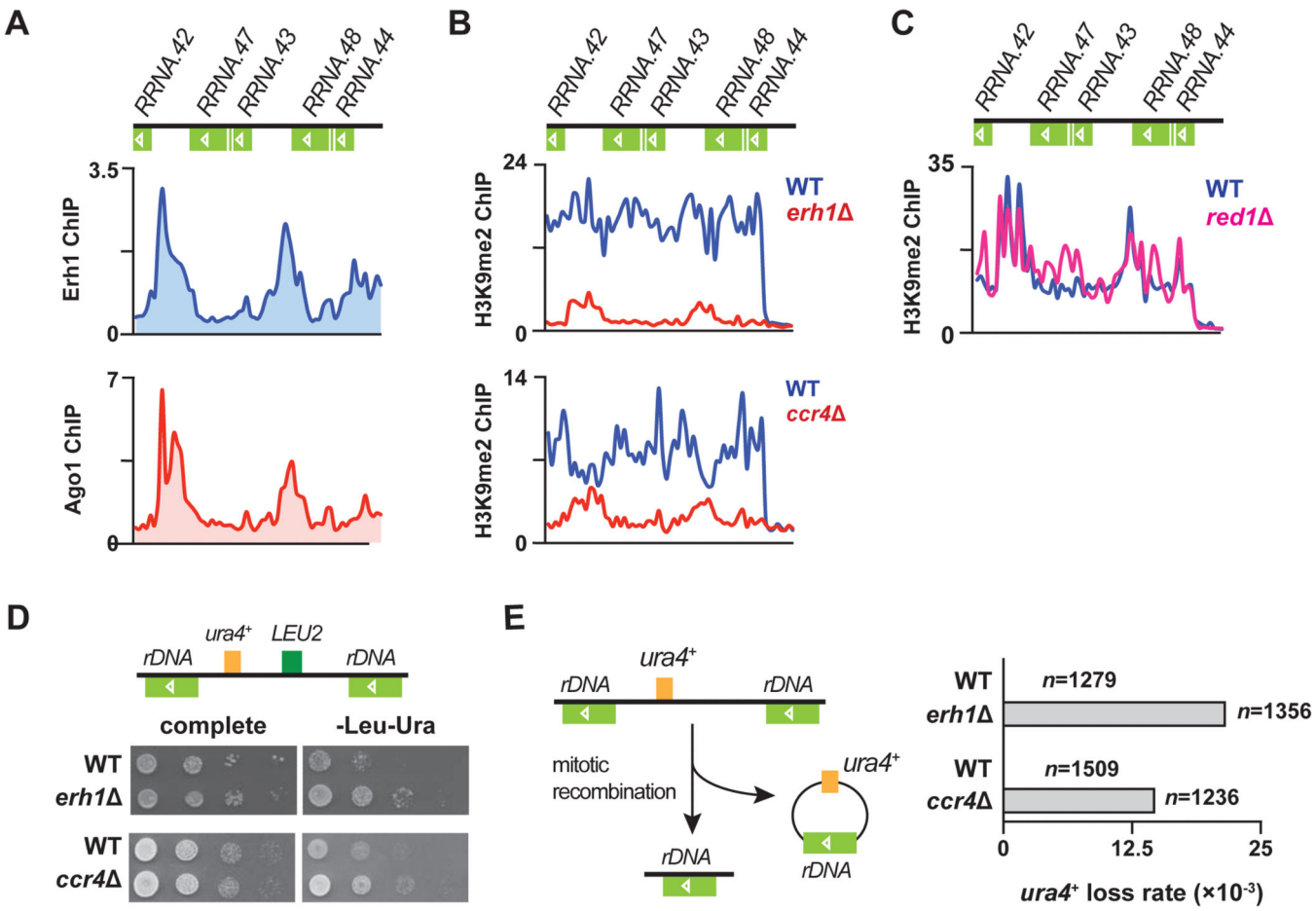

Figure 6. Erh1 and Ccr4 regulate heterochromatin formation at *rDNA* repeats to protect *rDNA* integrity

(A) ChIP-chip of Erh1-GFP (top) and myc-Ago1 (bottom) at *rDNA* repeats in WT. (B) ChIP-chip of H3K9me2 at *rDNA* repeats in WT and *erh1*Δ (top), and in WT and *ccr4*Δ (bottom). (C) ChIP-chip of H3K9me2 at *rDNA* repeats in WT and *red1*Δ. (D) *LEU2* and *ura4*$^+$ markers inserted at *rDNA* repeats (Ylp2.4pUC*ura4*$^+$-7) are de-repressed in *erh1*Δ and *ccr4*Δ. A schematic representation of Ylp2.4pUC*ura4*$^+$-7 is shown (top). WT and *erh1*Δ (middle) or WT and *ccr4*Δ (bottom) carrying Ylp2.4pUC*ura4*$^+$-7 were spotted onto complete medium or minimal medium lacking leucine and uracil (-Leu-Ura) and incubated at 30°C for 2 days. (E) Increased frequency of mitotic recombination at tandem *rDNA* repeats in *erh1*Δ and *ccr4*Δ. A schematic representation of *rDNA*::*ura4*$^+$ loss is shown (left). WT, *erh1*Δ and *ccr4*Δ carrying Ylp2.4pUC*ura4*$^+$-7 were first plated on medium lacking leucine, transferred to complete medium, and then replica plated to medium lacking uracil (-Ura). Mitotic recombination at *rDNA* loci was indicated by the lack of growth on -Ura plates, and was confirmed by genomic PCR. "*n*" indicates the number of cells counted for each strain. See also Figure S6.

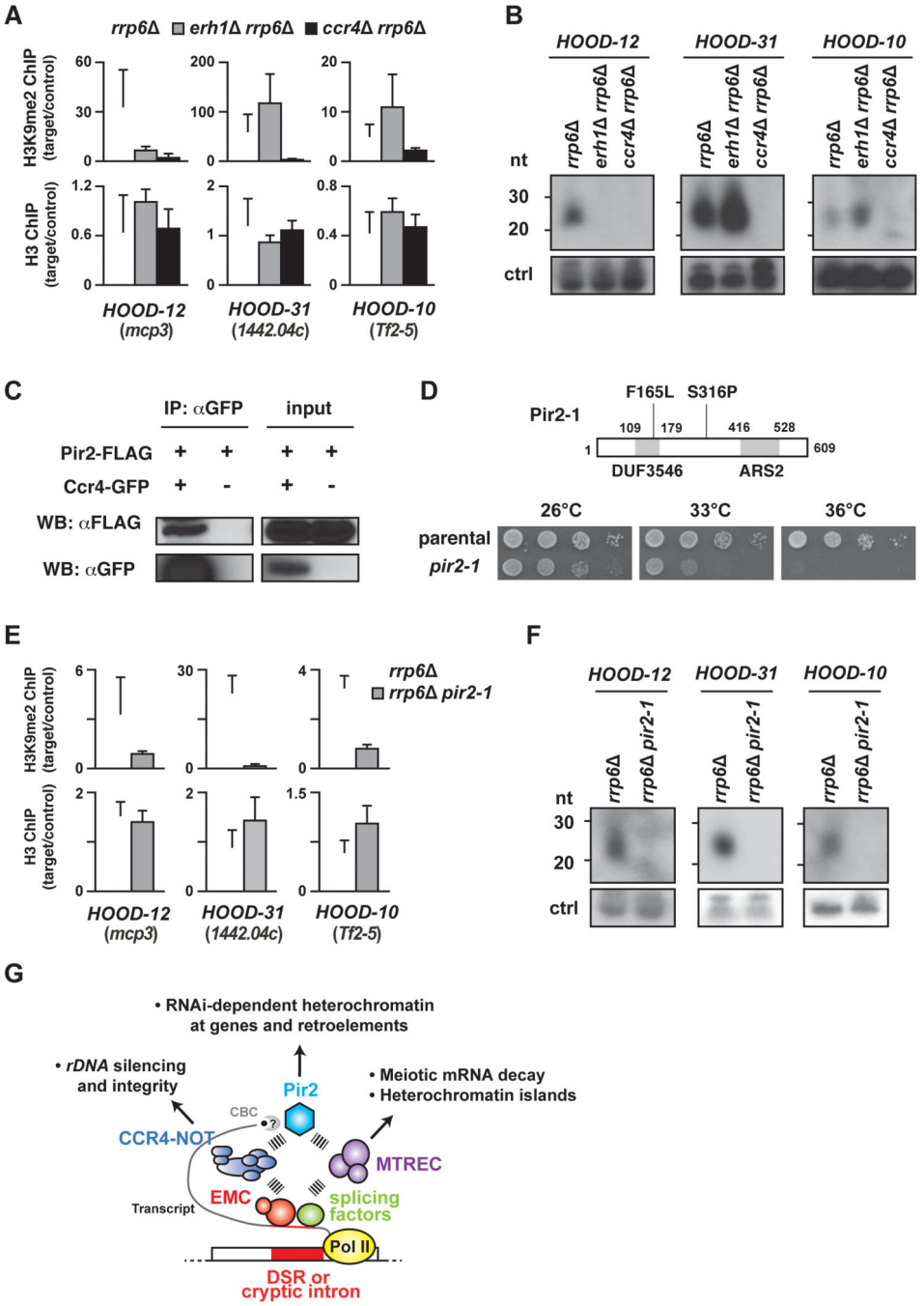

Figure 7. Ccr4 interacts with Pir2/ARS2 to promote small RNA production and H3K9 methylation at HOODs

(A) ChIP-qPCR of H3K9me2 and H3 at Mmi1-dependent (*HOOD-12*) and Mmi1-independent HOODs (*HOOD-31 and -10*) in *rrp6*Δ (white bars), *erh1*Δ *rrp6*Δ (grey bars) and *ccr4*Δ *rrp6*Δ (black bars). The fold enrichment values of the target loci relative to the control locus *vps33* are shown as the mean+SD (*n*=3). (B) Northern blot analysis of small RNA generation at three HOODs. Non-specific bands (~90 nt) served as a loading control (ctrl). (C) Co-immunoprecipitation of Pir2-FLAG with Ccr4-GFP. Cell lysates from the indicated strains were subjected to immunoprecipitation using anti-GFP antibody followed

by Western blotting. (D) Schematic showing the *pir2-1* allele, which encodes Pir2 protein containing Phe165 to Leu (F165L) and Ser316 to Pro (S316P) substitutions. Two conserved domains, DUF3546 and ARS2, are shown as grey boxes (top). Serial dilutions of parental wild-type (parental) and *pir2-1* cultures were spotted onto rich plates and then incubated at the indicated temperatures (bottom). (E) ChIP-qPCR of H3K9me2 and H3 at Mmi1-dependent (*HOOD-12*) and Mmi1-independent HOODs (*HOOD-31 and -10*) in *rrp6*Δ (white bars) and *rrp6*Δ *pir2-1* (grey bars). Fold enrichment of H3K9me2 and H3 at three target loci relative to the control locus (*vps33*) are shown as the mean+SD from three biological replicates. (F) Northern blot analysis of small RNAs generation at three HOODs. Non-specific bands (~90 nt) served as a loading control (ctrl). (G) Model showing EMC, CCR4-NOT, MTREC and Pir2 involvement in RNA-based regulation of gene expression and heterochromatin assembly. Transcripts containing a DSR are recognized by EMC, which in turn recruits MTREC and/or CCR4-NOT. MTREC is predominantly responsible for meiotic mRNA decay and formation of heterochromatin islands. On other hand, CCR4-NOT facilitates heterochromatin assembly at *rDNA* repeats and interacts with Pir2 (which also associates with Cap binding complex: CBC) and Pab2 (not depicted) to promote HOOD assembly at genes and retrotransposons. Pir2 is also known to associate with MTREC, implicated in formation of certain HOODs. In addition to the DSR, cryptic introns and splicing factors, which were previously implicated in the assembly of HOODs, likely also engage Pir2, CCR4-NOT and MTREC to promote mRNA decay and generate small RNAs mapping to HOODs. See also Figure S7.